Original Article | Gastrointestinal Imaging

eISSN 2005-8330
https://doi.org/10.3348/kjr.2020.1049
Korean J Radiol 2021;22(8):1300-1309

Korean Journal of Radiology
KJR

Quantification of Pancreas Surface Lobularity on CT: A Feasibility Study in the Normal Pancreas

Riccardo Sartoris[1, 2, 3], Alberto Calandra[1], Kyung Jin Lee[1, 4], Tobias Gauss[5], Valérie Vilgrain[1, 2, 3], Maxime Ronot[1, 2, 3]

[1]Department of Radiology, Hôpital Beaujon, Clichy, France; [2]Université de Paris, Paris, France; [3]INSERM U1149, Centre de Recherche de l'Inflammation (CRI), Paris, France; [4]Department of Radiology, Asan Medical Center, Seoul, Korea; [5]Intensive Care Unit, Hôpital Beaujon, Clichy, France

Objective: To assess the feasibility and reproducibility of pancreatic surface lobularity (PSL) quantification derived from abdominal computed tomography (CT) in a population of patients free from pancreatic disease.

Materials and Methods: This retrospective study included 265 patients free from pancreatic disease who underwent contrast-enhanced abdominal CT between 2017 and 2019. A maximum of 11 individual PSL measurements were performed by two abdominal radiologists (head [5 measurements], body, and tail [3 measurements each]) using dedicated software. The influence of age, body mass index (BMI), and sex on PSL was assessed using the Pearson correlation and repeated measurements. Inter-reader agreement was assessed using the intraclass correlation coefficient (ICC) and Bland Altman (BA) plots.

Results: CT images of 15 (6%) patients could not be analyzed. A total of 2750 measurements were performed in the remaining 250 patients (143 male [57%], mean age 45 years [range, 18–91]), and 2237 (81%) values were obtained in the head 951/1250 (76%), body 609/750 (81%), and tail 677/750 (90%). The mean ± standard deviation PSL was 6.53 ± 1.37. The mean PSL was significantly higher in male than in female (6.89 ± 1.30 vs. 6.06 ± 1.31, respectively, $p < 0.001$). PSL gradually increased with age ($r = 0.32$, $p < 0.001$) and BMI ($r = 0.32$, $p < 0.001$). Inter-reader agreement was excellent (ICC 0.82 [95% confidence interval 0.72–0.85], with a BA bias of 0.30 and 95% limits of agreement of -1.29 and 1.89).

Conclusion: CT-based PSL quantification is feasible with a high success rate and inter-reader agreement in subjects free from pancreatic disease. Significant variations were observed according to sex, age, and BMI. This study provides a reference for future studies.

Keywords: *Anatomy; Quantitative; Pancreatic lobule*

INTRODUCTION

According to the Quantitative Imaging Biomarkers Alliance, quantitative imaging involves "the extraction of quantifiable features from medical images for the assessment of normal or the severity, degree of change, or status of a disease, injury, or chronic condition relative to normal" [1]. Quantitative imaging allows for the validation of accurate image-derived parameters with anatomically and physiologically relevant meanings. Quantitative imaging is extensively used in modern medicine to improve diagnosis, assess prognosis, inform treatment selection, and monitor response to various treatments [2]. In oncology and abdominal disease, the response evaluation criteria in solid tumors [3,4] or liver stiffness measurements [5,6] are two examples of widely accepted and routinely used quantitative tools.

Organ contours may be modified by anatomical variants and physiological processes such as aging, or by various acute or chronic conditions and diseases. Imaging can visualize these changes, which may represent identifiable features to help radiologists reach or clarify diagnoses. One

Received: September 3, 2020 **Revised:** October 22, 2020
Accepted: November 3, 2020
Corresponding author: Maxime Ronot, MD, PhD, Department of Radiology, Hôpital Beaujon, 100 boulevard du Général Leclerc, 92110 Clichy, France.
• E-mail: maxime.ronot@aphp.fr

Korean Journal of Radiology
KJR

of the best examples is the liver capsule. In patients with chronic liver disease, the gradual development of fibrosis and regenerative hepatocellular nodules progressively leads to a nodular liver contour, and this qualitative or semi-quantitative sign has been shown to be highly specific for the diagnosis of cirrhosis [7-11]. Smith et al. [12,13] used a quantitative approach and showed that measurement of liver surface nodularity (LSN) on routine computed tomography (CT) images could accurately differentiate cirrhotic from non-cirrhotic livers [12] and could predict decompensated cirrhosis and death [13]. Since then, several studies have further validated this quantitative approach by showing its usefulness in detecting portal hypertension [14] or predicting short-term outcomes in patients undergoing liver resection [15].

In normal healthy subjects, the pancreas is a lobulated organ, a feature familiar to radiologists. Lobularity has been reported to increase with age [16]. Numerous focal or diffuse diseases, such as pancreatic cancer, autoimmune pancreatitis, diabetes, and locoregional treatments, such as radiotherapy, may also affect pancreas surface lobularity (PSL) on imaging [17-19]. Since the existing studies rely on visual assessment alone, the possible value of a more precise lobularity quantification remains unknown. Based on the quantitative approach introduced by Smith et al. [12,13] for the liver capsule, we hypothesized that PSL could be quantified through CT.

Thus, the aim of the current study was to assess the feasibility and reproducibility of PSL quantification derived from abdominal CT in a population of adult patients free from pancreatic disease to provide normal references for future clinical studies.

MATERIALS AND METHODS

Patient Population

This retrospective study, including a chart review, was approved by our Institutional Review Board; the requirement for written informed consent was waived (number CRM-2004-085). Patients with a normal pancreas were identified and extracted from the prospective trauma database of our on-site level 1 trauma center (highest level) between January 2016 and January 2019. Patients with any type of abdominal injury were excluded. Patients with clinical signs of severity (e.g., hemorrhagic shock) that could modify the appearance of the pancreas on CT were also excluded. Severity was defined as an Injury Severity Score of 4 or more [20]. Subsequently, a total of 394 consecutive patients were identified.

Care was then taken to exclude patients with a history of pancreatic disease or diabetes. To do so, medical charts were reviewed. Then, an abdominal radiologist retrospectively reviewed all CT examinations to exclude any patients with undetected abdominal traumatic injury or features of pancreatic disease, in particular calcifications, pancreatic duct dilation (> 5 mm), peripancreatic fat stranding, and focal pancreatic solid or cystic lesions. In addition, patients with a dysmorphic liver (i.e., liver nodularity, segment IV atrophy, or segment I hypertrophy) were excluded to avoid any type of chronic liver disease that might influence pancreas morphology. Ninety-five out of 394 patients were excluded because of the presence of previously unreported minor abdominal injuries (n = 34), pancreatic calcifications (n = 16), or pancreatic lesions (n = 45). None of the selected patients had a history of diabetes. To rule out possible unknown diabetes, we also excluded 27 patients with glycemia > 200 mg/dL at admission. Another 34 patients without available glycemia evaluations were excluded. The remaining 265 patients were considered for PSL quantification. Figure 1 shows a flowchart of the study population.

CT Protocol

Contrast-enhanced abdominal CT was performed on 128-section multi-detector CT scanners (Discovery CT750 HD LightSpeed, GE Healthcare). In our trauma center, the CT protocol included a contrast-enhanced acquisition obtained after intravenous administration of 2 mL/kg of non-ionic contrast medium at 350 mg iodine/mL with a power injector, through an 18-gauge catheter at a rate of 4 mL/s, and following a split-bolus injection protocol to obtain arterial and venous phase contrast on the same acquisition (nominal thickness, 0.625 mm; reconstruction thickness, 1.25 mm).

Pancreas Surface Lobularity Quantification

PSL was quantified by two abdominal radiologists using semi-automated CT software initially developed for LSN quantification (LSN software, version 0.88). To determine the mean attenuation of the pancreas (in order to calibrate the software for each patient), a circular region of interest (ROI) was drawn in the pancreatic head carefully excluding vessels or large areas of intrapancreatic fatty infiltration. If the size of the pancreatic head was not large enough, the ROI was drawn in the body or tail. Radiologists then

 https://doi.org/10.3348/kjr.2020.1049

painted a 1 cm diameter ROI across the anterior margin of the pancreas. The software automatically detected the pancreatic edge compared to adipose tissue on the selected section and on upward and downward continuous slices by propagating the painted ROI. The software automatically generated a smooth polynomial line to mimic a smooth pancreatic surface. The distance between the detected pancreatic margin and the polynomial line was measured on a pixel-by-pixel basis, expressed in tenths of a millimeter. Each ROI had to be at least 2.5 cm long to be used by the software. Measurements were performed in three different areas: head (five measurements), body and tail (three measurements each) following anatomical conventions [21], resulting in a maximum of 11 measurements obtained for each patient. Each individual measurement was considered to be successful if the software provided a value, and if the software did not include extra-pancreatic structures in its computation. If the software did not provide a value, the measurement was considered to be a failure. The value of each successful measurement was recorded for each patient, and the mean of the measurements was determined. Figure 2 shows an example of PSL quantification.

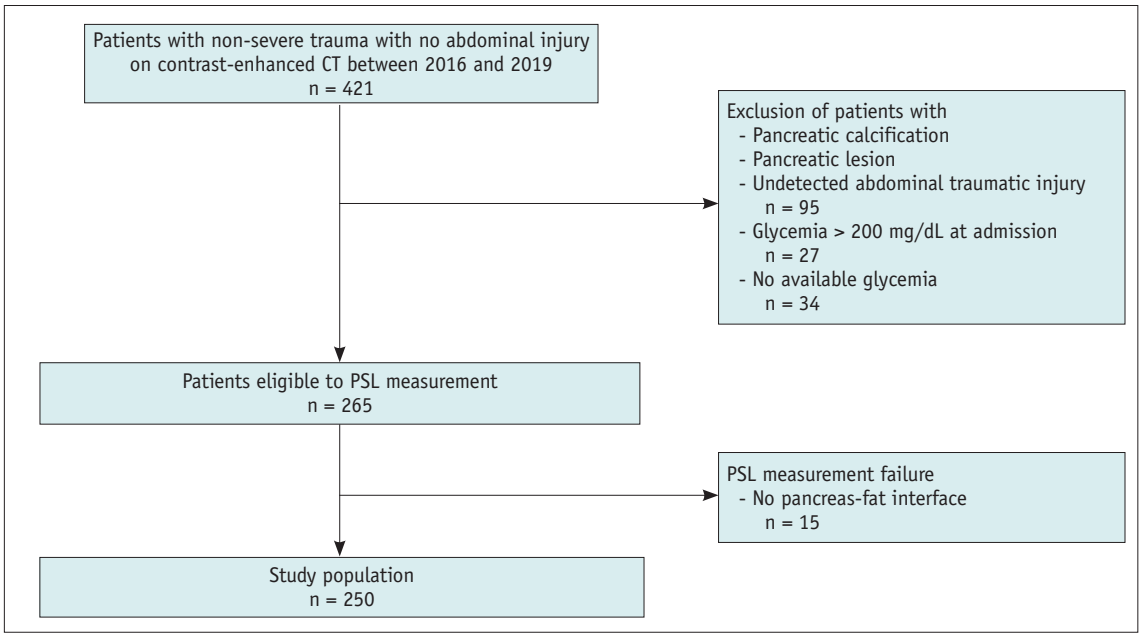

Fig. 1. Flowchart of the study. CT = computed tomography, PSL = pancreas surface lobularity

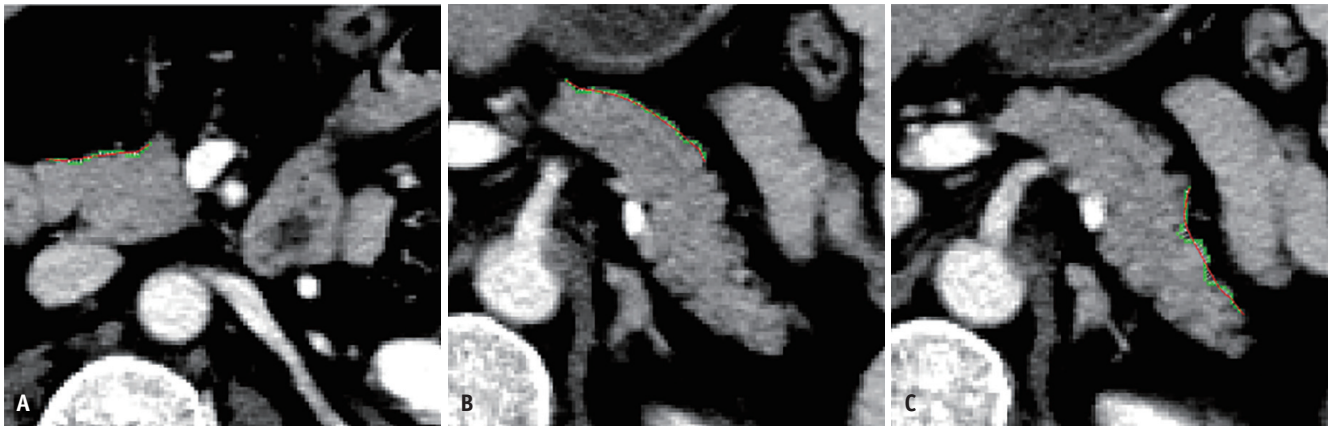

Fig. 2. Example of PSL measurement in a 41-year-old male patient.
A-C. Figures show magnified contrast enhanced computed tomography (single acquisition, split-bolus injection protocol) with measurement performed on the anterior margin of the head **(A)**, body **(B)**, and tail **(C)**, respectively. The software automatically generates smooth polynomial lines to mimic a smooth pancreatic surface (red lines) and detects the actual surface of the pancreas (green lines). The distance between the detected pancreatic margin and the polynomial line was measured on a pixel-by-pixel basis and expressed as tenths of a millimeter. The mean PSL score was 6.11. PSL = pancreas surface lobularity

https://doi.org/10.3348/kjr.2020.1049

Korean Journal of Radiology
KJR

Statistical Analysis

Continuous variables are expressed as means ± standard deviations and were compared using the Student *t* test or Mann-Whitney test, and the ANOVA or Kruskal-Wallis tests, when appropriate. Comparison of measurements in the same patients required paired tests and mixed-effects models in case of multiple comparisons. The Gaussian distribution of the included variables was tested using the Kolmogorov-Smirnov test. Comparisons between categorical variables were performed using the chi-square test or Fisher's exact test, when appropriate. Correlations were computed using Pearson's correlation coefficient.

Inter-reader variability was assessed by the intraclass correlation coefficient (ICC) and the Bland-Altman plot. The ICC agreement was based on the Landis and Koch benchmark for Kappa agreement [22], with results of < 0.2 regarded as slight agreement, 0.2–0.4 as fair, 0.41–0.6 as moderate, 0.61–0.8 as substantial, and 0.81–1 as excellent. The 95% confidence interval (CI) was calculated.

All tests were two-sided and a *p* value less than 0.05 was considered to be statistically significant. Statistical analyses and figures were performed using the MedCalc software (v19.0.7, MedCalc Software Ltd.), SPSS statistical package 25.0 software (IBM Corp.) and GraphPad Prism 8 software (GraphPad Software Inc.).

RESULTS

Feasibility of Pancreas Surface Lobularity Measurement

Fifteen patients (6%) could not be analyzed using the software due to an insufficient pancreas-fat interface. The remaining 250 patients included 143 male, mean age 43 years (18–81 years), and 107 female (mean age, 47 years) (18-91 years). The overall mean age of patients was 45 years (range, 18–91 years). The mean BMI was 24.9 ± 4.2 kg/m^2, and was not significantly different between male and female (mean 25.2 ± 4.0 vs. 24.6 ± 4.4 kg/m^2, respectively, $p = 0.277$).

A total of 2750 individual measurements were performed, and 2237 (81%) of these were successful. There were 951/1250 (76%), 609/750 (81%), and 677/750 (90%) successful measurements in the head, body, and tail, respectively.

Table 1 shows the distribution of patients according to the number of successful individual PSL measurements. The median number of successful measurements per patient was 10 (range, 1–11). At least three successful measurements were obtained in 245/250 patients (98%). A total of 198/250 (79%), 184/250 (74%), and 211/250 (84%) patients had three successful measurements or more in the head, body, and tail, respectively ($p < 0.001$). Overall, 108/250 patients (43%) had 11 successful measurements.

Pancreas Surface Lobularity Quantification

Details of the PSL are provided in Table 2. The PSL for the entire cohort was 6.53 ± 1.37. When considering the 245 patients with ≥ 3 individual measurements in the whole pancreas, the mean PSL 6.53 ± 1.37. The mean time to obtain measurements was 240 ± 113 seconds. PSL was obtained in the head, body, and tail in 226/250, 218/250, and 236/250 patients, respectively ($p < 0.001$). The mixed-effects model showed significant within-patient differences between PSL in the head, body, and tail ($p < 0.001$, pairwise post hoc comparisons $p = 0.007$ to $p < 0.001$). PSL

Table 1. Distribution of the 250 Patients according to the Number of Successful Individual Pancreas Surface Lobularity Measurements Obtained in the Head (From 0 to 5), the Body (From 0 to 3), and Tail (From 0 to 3) and All Together (From 0 to 11)

Measurements	Head	Body	Tail	Head + Body + Tail
0	24 (10)	32 (13)	14 (6)	0 (-)
1	9 (4)	11 (4)	6 (2)	2 (1)
2	19 (8)	23 (9)	19 (8)	3 (2)
3	24 (10)	184 (74)	211 (84)	4 (2)
4	38 (15)			3 (2)
5	136 (54)			6 (4)
6				11 (7)
7				7 (4)
8				17 (10)
9				12 (7)
10				22 (13)
11				77 (47)

Data are presented as patients number (%).

https://doi.org/10.3348/kjr.2020.1049

Table 2. PSL Measurement according to Age and Sex

	PSL Total	PSL Head	PSL Body	PSL Tail	*P**
Total	6.53 ± 1.37	6.43 ± 1.58	6.07 ± 1.63	7.28 ± 1.37	< 0.001
Male	6.89 ± 1.30	6.74 ± 1.61	6.37 ± 1.69	7.84 ± 1.95	< 0.001
Female	6.06 ± 1.31	5.97 ± 1.42	5.66 ± 1.20	6.51 ± 1.99	< 0.001
p value†	< 0.001	< 0.001	< 0.001	< 0.001	
Correlation with age					
r (*p* value)	0.32 (< 0.001)	0.35 (< 0.001)	0.18 (0.008)	0.24 (< 0.001)	
Age category					
18–30 years (n = 69)	5.95 ± 1.05	5.76 ± 1.13	5.63 ± 1.21	6.56 ± 1.91	< 0.001
Male (n = 40)	6.32 ± 0.96	6.03 ± 1.07	6.06 ± 1.13	7.24 ± 1.96	0.001
Female (n = 29)	5.43 ± 0.94	5.36 ± 1.13	5.13 ± 0.88	5.71 ± 1.48	0.060
p value†	0.0003	0.022	0.004	0.001	
31–50 years (n = 75)	6.43 ± 1.08	6.20 ± 1.29	5.99 ± 1.61	7.12 ± 1.95	< 0.001
Male (n = 50)	6.72 ± 1.02	6.43 ± 1.39	6.25 ± 1.51	7.57 ± 1.72	< 0.001
Female (n = 25)	5.86 ± 0.99	5.64 ± 0.78	5.41 ± 1.71	6.17 ± 2.10	0.042
p value†	< 0.001	0.019	0.051	0.004	
51–70 years (n = 86)	6.98 ± 1.48	6.95 ± 1.61	6.36 ± 1.79	7.85 ± 2.00	< 0.001
Male (n = 46)	7.39 ± 1.48	7.43 ± 1.58	6.62 ± 1.99	8.41 ± 1.94	< 0.001
Female (n = 40)	6.51 ± 1.34	6.39 ± 1.47	6.04 ± 1.47	7.22 ± 1.92	< 0.001
p value†	0.005	0.004	0.154	0.007	
71 years and older (n = 20)	7.06 ± 1.94	7.24 ± 2.48	6.41 ± 1.78	7.64 ± 2.60	0.084
Male (n = 7)	8.12 ± 1.76	8.72 ± 2.83	7.12 ± 2.06	9.32 ± 2.26	0.229
Female (n = 13)	6.49 ± 1.85	6.51 ± 2.03	6.05 ± 1.59	6.66 ± 2.32	0.481
p value§	0.115	0.125	0.423	0.023	
p value total‡	< 0.001	< 0.001	0.060	0.002	
p value male‡	< 0.001	< 0.001	0.343	0.006	
p value female‡	0.003	0.013	0.061	0.015	

**p* value for the row comparison between head, body and tail, mixed-effects model, †*p* value for the comparison between sex per age category, *t* test, ‡*p* value for the comparison between age categories, ANOVA, §*p* value for the comparison between sex per age category, Mann-Whitney. PSL = pancreas surface lobularity

was significantly higher in the tail than in other parts of the pancreas.

Relation with Age

PSL was moderately and significantly correlated with age for the entire pancreas ($r = 0.32$, $p < 0.001$). Correlations were also observed for each of the separate parts of the pancreas. The correlation was stronger in the head ($r = 0.35$, $p < 0.001$) and weaker in the body ($r = 0.18$, $p = 0.008$) (Fig. 3).

After patient stratification by age category (18–30 years [69 patients]; 31–50 years [75 patients]; 51–70 years [86 patients], and 71+ years [20 patients]), the mean PSL was shown to gradually increase with age (mean 5.95 ± 1.05, 6.43 ± 1.08, 6.98 ± 1.48, and 7.06 ± 1.94, respectively, $p < 0.001$). This remained significant in male and female ($p < 0.001$ and $p = 0.003$, respectively). It was also significant when considering the pancreatic head or tail (totally and in male and female, separately). The results in the body neared significance ($p = 0.060$) (Table 2, Fig. 4).

Relation with BMI

PSL was moderately and significantly correlated with BMI for the entire pancreas ($r = 0.32$, $p < 0.001$). The correlation was stronger in male ($r = 0.40$, $p < 0.001$) than in female ($r = 0.21$, $p = 0.031$) (Fig. 5).

After patient stratification by BMI categories (i.e., < 18.5, 18.5–24.9, 25–29.9, and ≥ 30 kg/m^2), the mean PSL in the entire pancreas gradually increased with the BMI categories ($p < 0.001$). This was also true for the pancreatic head ($p = 0.002$) and body ($p = 0.003$), but not the tail ($p = 0.234$) (Fig. 5). BMI was weakly but significantly correlated with age ($r = 0.19$, $p = 0.003$), and PSL appeared to be co-associated with both age and BMI. Figure 6 shows the progressive increase in PSL with age and BMI.

https://doi.org/10.3348/kjr.2020.1049

Korean Journal of Radiology
KJR

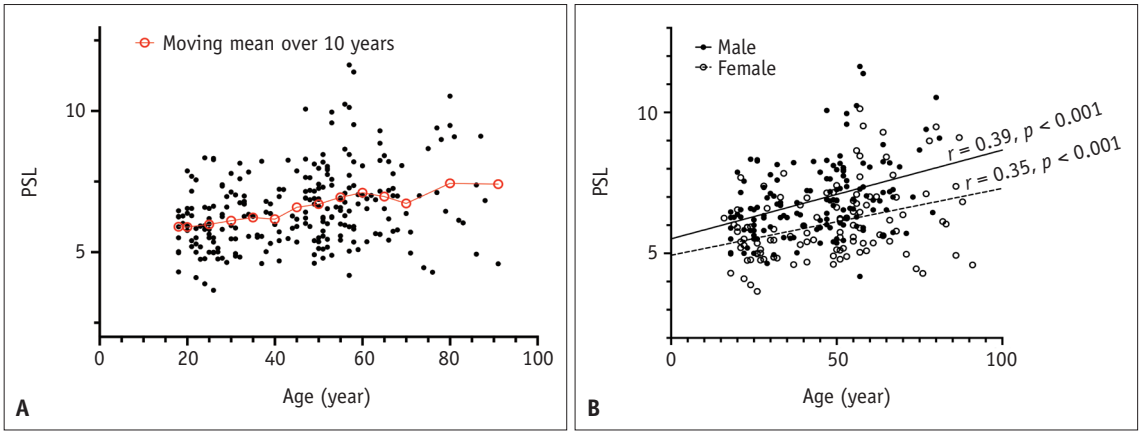

Fig. 3. Distribution of PSL according to age.
A. Overall distribution of the entire cohort, the red line corresponds to the sliding PSL average over ten years, and shows a progressive increase of PSL with age. **B.** Difference between male (black dots), and female (white dots). In both groups, PSL was significantly correlated with age (r = 0.39, p < 0.001 in male and r = 0.35, p < 0.001 in female). PSL = pancreas surface lobularity

Relation with Sex

PSL was significantly higher in male than in female (mean 6.89 ± 1.30 vs. 6.06 ± 1.31, p < 0.001). This was also true for each part of the pancreas taken separately (all p < 0.001). The mean PSL in the head, body, and tail were significantly different in both male and female (p < 0.001), with PSL values found to be significantly higher in the tail than in other parts of the pancreas. Supplementary Table 1 compares the results in male and female with similar ages and BMI categories.

Inter-Observer Agreement

The measurements of the two readers were strongly correlated (r = 0.81, p < 0.001). Inter-reader agreement was excellent, with an ICC of 0.82 (95% CI 0.72–0.85, p < 0.001). The Bland-Altman plot showed a systematic bias of 0.30 with 95% limits of agreement of -1.29 and 1.89 (Table 3, Supplementary Fig. 1). Inter-reader variability was higher for measurements in the body of the pancreas (ICC 0.37 [95% CI 0.18–0.53], bias 1.53, with 95% limits of agreement of -2.27 and 5.34) than for other parts of the pancreas.

DISCUSSION

This study assessed the feasibility and reproducibility of PSL quantification on CT images in a population of adult patients free from pancreatic disease. Our results show that PSL quantification was highly feasible and associated with excellent inter-reader agreement. PSL was influenced by sex and increased with both age and BMI.

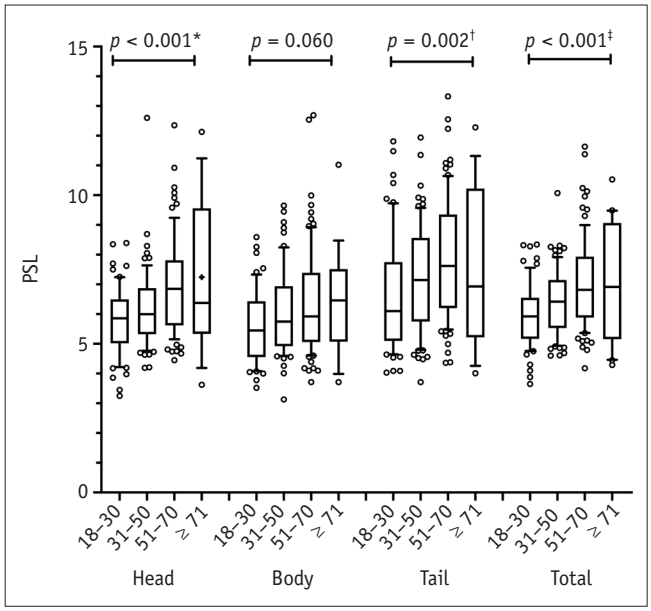

Fig. 4. Box plots representing the distribution of PSL according to age categories (i.e. 18–30, 31–50, 51–70, and 71 or more years old), in the head, body and tail of the pancreas, and for the entire pancreas. PSL was found to significantly increase with age in all parts of the pancreas, except in the body. Boxes represent the 10th–90th percentile, whiskers 1st–99th percentile, and dots are outliers. The central bar represents the median. Post-hoc comparisons: *Head: all paired comparisons were significant except for 18–30 vs. 31–50 and 51–70 vs. ≥ 71, †Tail: only 18–30 vs. 51–70 found significant. Other paired comparisons were not significant, ‡All: 18–30 vs. 51–70, 18–30 vs. ≥ 71 and 31–50 vs. 51–70 were found significant. Other paired comparisons were not significant. PSL = pancreas surface lobularity

Overall, PSL quantification was shown to be highly feasible. These results are interesting because the software we used was created to quantify the nodularity of the liver capsule [12], rather than the contours of the pancreas. This

https://doi.org/10.3348/kjr.2020.1049

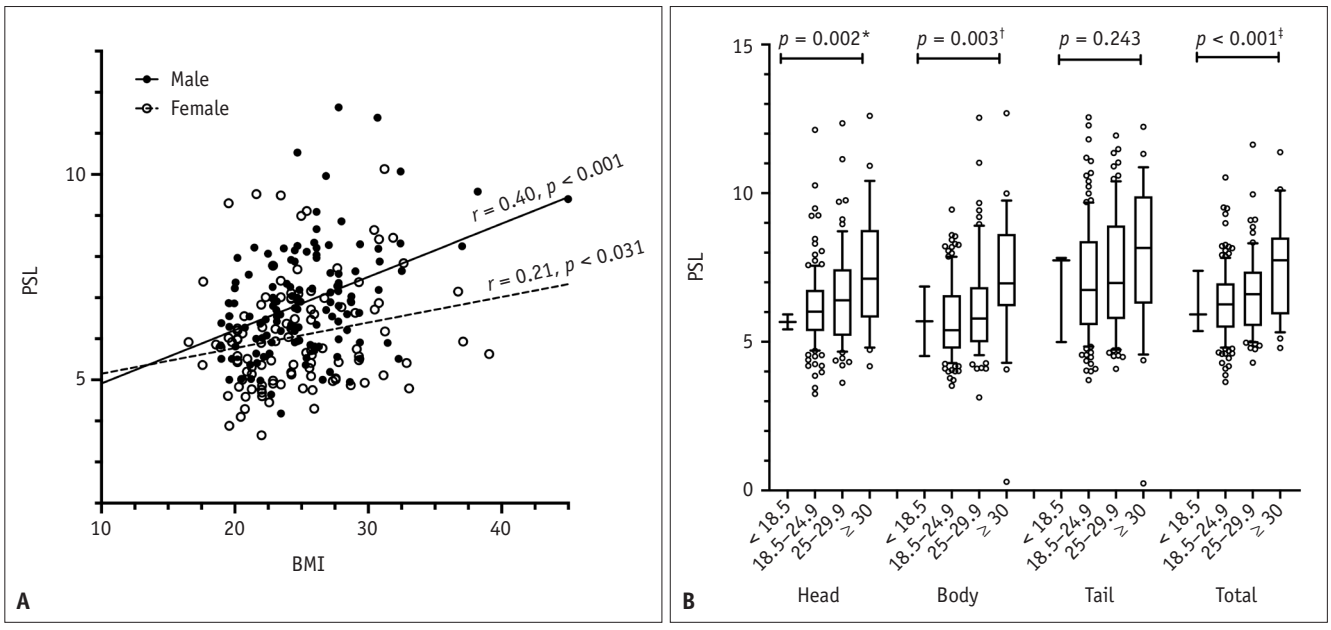

Fig. 5. Distribution of PSL according to BMI.
A. shows the difference between male (black dots) and female (white dots). In both groups, PSL was significantly correlated with BMI, but the correlation was stronger in male ($r = 0.40$, $p < 0.001$) than in female ($r = 0.21$, $p < 0.031$). **B.** Box plots representing the distribution of PSL according to BMI categories (i.e., < 18.5, 18.5–24.9, 25–29.9, and ≥ 30 kg/m^2), head, body, and tail of the pancreas, and in the entire pancreas. PSL was found to significantly increase with BMI categories in all parts of the pancreas. Boxes represent the 10th–90th percentile, whiskers 1st–99th percentile, and dots are outliers. The central bar represents the median. Post-hoc comparisons: *Head: only 18.5–24.9 vs. ≥ 30 was significant, †Body: only 18.5–24.9 vs. ≥ 30 was significant, ‡All: 18.5–24.9 vs. ≥ 30 and 25–29.9 vs. ≥ 30 were significant. BMI = body mass index, PSL = pancreas surface lobularity

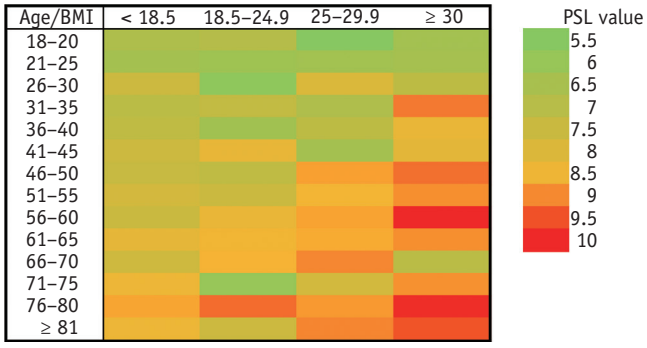

Fig. 6. Heat map representing PSL values according to age (by increment of 5 years) and BMI categories (i.e. < 18.5, 18.5–24.9, 25–29.9, and ≥ 30 kg/m^2). The map shows the progressive increase of PSL with both age and BMI. BMI = body mass index, PSL = pancreas surface lobularity

Table 3. Inter-Reader Agreement for PSL Measurements

	ICC (95% CI)	Bland Altman		
		Bias	95% Lower LOA	95% Upper LOA
PSL				
Total	0.81 (0.74–0.86)	0.30	-1.29	1.89
Head	0.74 (0.78–0.90)	0.27	-1.89	2.43
Body	0.37 (0.18–0.53)	1.53	-2.27	5.34
Tail	0.74 (0.64–0.81)	-0.35	-2.94	2.23

CI = confidence interval, ICC = intraclass correlation coefficient, LOA = limits of agreement, PSL = pancreas surface lobularity

software works by identifying the organ-fat interface; thus, we hypothesized that it could be applied to other organs with similar conspicuous contours, such as the pancreas. These results validate this hypothesis because the technical success rate was 94%, and only 15 patients had complete measurement failures due to an insufficient pancreas-fat interface. Noticeably, technical failure was not due to the architecture of the software itself, but rather to anatomical structures (e.g., gastroduodenal artery in the head, contact with the pyloric region or with the small gastric curve for the isthmus and body, or a tortuous splenic artery on the tail) that modified the pancreas contours and the pancreas-fat interface. We arbitrarily chose to perform 11 individual measurements per patient, separating the head, body, and tail of the pancreas, to sample as much of the pancreas as possible, and to assess possible differences in the parts of the organ. The software provided a numerical value for 80% of the measurements, and most of the patients had at least three measurements. It is important to note that there were significantly fewer successful measurements in the body of the pancreas. Overall, inter-reader agreement was also found

https://doi.org/10.3348/kjr.2020.1049

Korean Journal of Radiology
KJR

to be excellent, but was only fair in the body. One possible explanation is that the stomach presses against the anterior margin of the body of the pancreas, degrading the organ-fat interface and increasing the number of failures and inter-reader variability. Although these results could be important in defining the quality criteria of PSL measurements, this was not a goal in this exploratory study of patients free from pancreatic disease. Quality criteria must be determined and validated in relation to clinically relevant endpoints [23]. Nevertheless, our results suggest that measurements should focus on the tail and head rather than the body of the pancreas.

Histological changes in the pancreas, particularly fibrosis, fatty replacement, and lobulocentric pancreatic atrophy, are known to occur with age [24]. Pancreatic lobulation is probably associated with these modifications and may be more easily visualized on the border of the pancreas. This would explain the age-related increase in lobularity on both CT [25] and MRI [16], which is confirmed by our study showing that PSL is positively correlated to and significantly increases with age and age categories. This is true in both male and female and in all parts of the pancreas, except in the body. PSL was also shown to be positively correlated with BMI and to significantly increase with BMI categories. We believe these results should be interpreted in relation to the well-known modifications in the histology and volume of the pancreas in overweight or obese patients [26-28]. Altogether, the co-association of age and BMI with PSL suggests that this feature may reflect significant histological changes, especially the fatty infiltration of the gland. If these results are confirmed by radio-pathological studies, this could support the clinical value of PSL.

Indeed, our study was performed in patients free from pancreatic disease, but histological changes in the pancreas are known to be associated with diabetes [29], carcinogenesis [26], or postoperative complications [30]. Kim et al. [31] Lim et al. [32] used different approaches to demonstrate the association of CT-based quantitative assessment of pancreatic fat with impaired glucose metabolism, while Jang et al. [33] demonstrated the value of CT texture analysis of the pancreas in predicting diabetes. These studies suggest that non-invasive quantitative evaluation of the pancreatic parenchyma on CT could be clinically useful. We believe that our study provides a reference for normal PSL to perform further clinical studies.

Our study showed for the first time that PSL significantly varied in the different parts of the pancreas, with higher values in the tail. These results confirm the impression of radiologists and surgeons and suggest that measurements should be performed in similar parts of the pancreas over time to avoid errors. More surprising were the consistently lower PSL values in female compared to men. Although one could imagine that these sex disparities reflected differences in BMI or age in the cohort, the mean age and BMI of male and female were similar. While performing a sub-group comparison of sex with similar age and BMI categories was more difficult to interpret because of the small number of patients available for these analyses, sex differences were confirmed in several cases. One explanation is the possible unknown differences in medical histories that may have affected the structure of the pancreas. We excluded patients with a history of diabetes and those with calcified peripancreatic arteries but other conditions, for example, dyslipidemia or mild atherosclerosis, could have resulted in chronic microscopic changes in the pancreatic parenchyma, and therefore have influenced our results. Visceral fat seems to be correlated to the fatty replacement of the pancreas, and its association with PSL should be investigated to address sex-related differences [34,35].

Our study has certain limitations. In addition to its retrospective design, as mentioned above, we did not perform radio-pathological correlations. Thus, we could not compare CT-derived PSL with clinically significant histological lesions affecting the pancreas, such as fibrosis, fat, or pancreatic intraepithelial neoplasia. This investigation is needed for a better understanding of the PSL value. Second, certain conditions such as alcohol intake were not evaluated because of the retrospective selection of patients, and may have influenced the results, even if exclusion criteria included visual signs of potential chronic alcohol intake (pancreatic calcifications and liver morphology). Third, PSL was only assessed on CT. Other imaging techniques that are frequently performed in patients with pancreatic disease, especially qualitative or quantitative MR imaging, require specific studies.

In conclusion, we showed that CT-based PSL quantification is feasible with a high success rate and with high inter-reader agreement in patients free from pancreatic disease. PSL was found to be higher in male, and gradually increased with both age and BMI. The study provides reference for further investigations assessing the diagnostic and prognostic value of PSL in various clinical contexts, such as diabetes, pancreatitis, or in the initial work-up of

 https://doi.org/10.3348/kjr.2020.1049

patients undergoing pancreas resection.

Supplement

The Supplement is available with this article at https://doi.org/10.3348/kjr.2020.1049.

Conflicts of Interest

The authors have no potential conflicts of interest to disclose.

Author Contributions

Conceptualization: Maxime Ronot. Data curation: Riccardo Sartoris, Alberto Calandra, Kyung Jin Lee, Tobias Gauss. Formal analysis: Maxime Ronot, Riccardo Sartoris. Methodology: Maxime Ronot. Project administration: Maxime Ronot, Valérie Vilgrain. Resources: Maxime Ronot, Valérie Vilgrain. Supervision: Maxime Ronot. Validation: Maxime Ronot. Writing—original draft: Riccardo Sartoris, Alberto Calandra, Maxime Ronot. Writing—review & editing: all authors.

ORCID iDs

Riccardo Sartoris
https://orcid.org/0000-0001-5890-0341
Alberto Calandra
https://orcid.org/0000-0002-8408-3557
Kyung Jin Lee
https://orcid.org/0000-0003-2607-9792
Tobias Gauss
https://orcid.org/0000-0003-0056-8192
Valérie Vilgrain
https://orcid.org/0000-0002-3568-7725
Maxime Ronot
https://orcid.org/0000-0001-7464-3939

REFERENCES

1. RSNA. Quantitative imaging biomarkers alliance. Rsna.org Web site. https://www.rsna.org/en/research/quantitative-imaging-biomarkers-alliance. Accessed June 7, 2020
2. Rosenkrantz AB, Mendiratta-Lala M, Bartholmai BJ, Ganeshan D, Abramson RG, Burton KR, et al. Clinical utility of quantitative imaging. *Acad Radiol* 2015;22:33-49
3. Eisenhauer EA, Therasse P, Bogaerts J, Schwartz LH, Sargent D, Ford R, et al. New response evaluation criteria in solid tumours: revised RECIST guideline (version 1.1). *Eur J Cancer* 2009;45:228-247
4. Therasse P, Arbuck SG, Eisenhauer EA, Wanders J, Kaplan RS, Rubinstein L, et al. New guidelines to evaluate the response to treatment in solid tumors. European Organization for Research and Treatment of Cancer, National Cancer Institute of the United States, National Cancer Institute of Canada. *J Natl Cancer Inst* 2000;92:205-216
5. de Franchis R; Baveno VI Faculty. Expanding consensus in portal hypertension: report of the Baveno VI Consensus Workshop: stratifying risk and individualizing care for portal hypertension. *J Hepatol* 2015;63:743-752
6. European Association for Study of Liver; Asociacion Latinoamericana para el Estudio del Higado. EASL-ALEH Clinical Practice Guidelines: non-invasive tests for evaluation of liver disease severity and prognosis. *J Hepatol* 2015;63:237-264
7. Berzigotti A, Ashkenazi E, Reverter E, Abraldes JG, Bosch J. Non-invasive diagnostic and prognostic evaluation of liver cirrhosis and portal hypertension. *Dis Markers* 2011;31:129-138
8. Goyal N, Jain N, Rachapalli V, Cochlin DL, Robinson M. Non-invasive evaluation of liver cirrhosis using ultrasound. *Clin Radiol* 2009;64:1056-1066
9. Romero M, Palmer SL, Kahn JA, Ihde L, Lin LM, Kosco A, et al. Imaging appearance in acute liver failure: correlation with clinical and pathology findings. *Dig Dis Sci* 2014;59:1987-1995
10. Colli A, Fraquelli M, Andreoletti M, Marino B, Zuccoli E, Conte D. Severe liver fibrosis or cirrhosis: accuracy of US for detection--analysis of 300 cases. *Radiology* 2003;227:89-94
11. Gaiani S, Gramantieri L, Venturoli N, Piscaglia F, Siringo S, D'Errico A, et al. What is the criterion for differentiating chronic hepatitis from compensated cirrhosis? A prospective study comparing ultrasonography and percutaneous liver biopsy. *J Hepatol* 1997;27:979-985
12. Smith AD, Branch CR, Zand K, Subramony C, Zhang H, Thaggard K, et al. Liver surface nodularity quantification from routine CT images as a biomarker for detection and evaluation of cirrhosis. *Radiology* 2016;280:771-781
13. Smith AD, Zand KA, Florez E, Sirous R, Shlapak D, Souza F, et al. Liver surface nodularity score allows prediction of cirrhosis decompensation and death. *Radiology* 2017;283:711-722
14. Sartoris R, Rautou PE, Elkrief L, Pollorsi G, Durand F, Valla D, et al. Quantification of liver surface nodularity at CT: utility for detection of portal hypertension. *Radiology* 2018;289:698-707
15. Hobeika C, Cauchy F, Sartoris R, Beaufrère A, Yoh T, Vilgrain V, et al. Relevance of liver surface nodularity for preoperative risk assessment in patients with resectable hepatocellular carcinoma. *Br J Surg* 2020;107:878-888
16. Sato T, Ito K, Tamada T, Sone T, Noda Y, Higaki A, et al. Age-related changes in normal adult pancreas: MR imaging evaluation. *Eur J Radiol* 2012;81:2093-2098
17. Prokesch RW, Chow LC, Beaulieu CF, Bammer R, Jeffrey RB Jr. Isoattenuating pancreatic adenocarcinoma at multi-detector

row CT: secondary signs. *Radiology* 2002;224:764-768
18. Manfredi R, Graziani R, Cicero C, Frulloni L, Carbognin G, Mantovani W, et al. Autoimmune pancreatitis: CT patterns and their changes after steroid treatment. *Radiology* 2008;247:435-443
19. Gilbeau JP, Poncelet V, Libon E, Derue G, Heller FR. The density, contour, and thickness of the pancreas in diabetics: CT findings in 57 patients. *AJR Am J Roentgenol* 1992;159:527-531
20. Linn S. The injury severity score--importance and uses. *Ann Epidemiol* 1995;5:440-446
21. Netter FH. *Atlas of human anatomy*, 5th ed. Philadelphia: Saunders, 2014:277-282
22. Landis JR, Koch GG. The measurement of observer agreement for categorical data. *Biometrics* 1977;33:159-174
23. Sartoris R, Lazareth M, Nivolli A, Dioguardi Burgio M, Vilgrain V, Ronot M. CT-based liver surface nodularity for the detection of clinically significant portal hypertension: defining measurement quality criteria. *Abdom Radiol (NY)* 2020;45:2755-2763
24. Matsuda Y. Age-related morphological changes in the pancreas and their association with pancreatic carcinogenesis. *Pathol Int* 2019;69:450-462
25. Heuck A, Maubach PA, Reiser M, Feuerbach S, Allgayer B, Lukas P, et al. Age-related morphology of the normal pancreas on computed tomography. *Gastrointest Radiol* 1987;12:18-22
26. Rebours V, Gaujoux S, d'Assignies G, Sauvanet A, Ruszniewski P, Lévy P, et al. Obesity and fatty pancreatic infiltration are risk factors for pancreatic precancerous lesions (PanIN). *Clin Cancer Res* 2015;21:3522-3528
27. Saisho Y, Butler AE, Meier JJ, Monchamp T, Allen-Auerbach M, Rizza RA, et al. Pancreas volumes in humans from birth to age one hundred taking into account sex, obesity, and presence of type-2 diabetes. *Clin Anat* 2007;20:933-942
28. DeSouza SV, Singh RG, Yoon HD, Murphy R, Plank LD, Petrov MS. Pancreas volume in health and disease: a systematic review and meta-analysis. *Expert Rev Gastroenterol Hepatol* 2018;12:757-766
29. Khoury T, Asombang AW, Berzin TM, Cohen J, Pleskow DK, Mizrahi M. The clinical implications of fatty pancreas: a concise review. *Dig Dis Sci* 2017;62:2658-2667
30. Mathur A, Pitt HA, Marine M, Saxena R, Schmidt CM, Howard TJ, et al. Fatty pancreas: a factor in postoperative pancreatic fistula. *Ann Surg* 2007;246:1058-1064
31. Kim SY, Kim H, Cho JY, Lim S, Cha K, Lee KH, et al. Quantitative assessment of pancreatic fat by using unenhanced CT: pathologic correlation and clinical implications. *Radiology* 2014;271:104-112
32. Lim S, Bae JH, Chun EJ, Kim H, Kim SY, Kim KM, et al. Differences in pancreatic volume, fat content, and fat density measured by multidetector-row computed tomography according to the duration of diabetes. *Acta Diabetol* 2014;51:739-748
33. Jang S, Kim JH, Choi SY, Park SJ, Han JK. Application of computerized 3D-CT texture analysis of pancreas for the assessment of patients with diabetes. *PLoS One* 2020;15:e0227492
34. Ozbulbul NI, Yurdakul M, Tola M. Does the visceral fat tissue show better correlation with the fatty replacement of the pancreas than with BMI? *Eurasian J Med* 2010;42:24-27
35. Singh RG, Cervantes A, Kim JU, Nguyen NN, DeSouza SV, Dokpuang D, et al. Intrapancreatic fat deposition and visceral fat volume are associated with the presence of diabetes after acute pancreatitis. *Am J Physiol Gastrointest Liver Physiol* 2019;316:G806-G815

 https://doi.org/10.3348/kjr.2020.1049